



Experimental and Numerical Investigation of Load Carrying Capacity of Vertically and Horizontally Reinforced Floating Stone Column Group

Ankit Thakur · Saurabh Rawat · Ashok Kumar Gupta

Received: 29 April 2020 / Accepted: 13 December 2020 / Published online: 2 January 2021
© The Author(s), under exclusive licence to Springer Nature Switzerland AG part of Springer Nature 2021

Abstract The present work investigates the load carrying capacity of vertically and horizontally reinforced floating stone column group through model testing. Two group arrangements using three and four stone columns for both unreinforced and reinforced conditions are testing under compressive loading. The geotextile reinforcement is provided throughout the stone column length (300 mm) in vertical direction and in form of circular discs at spacing of 30 mm along column length for reinforcing horizontally. The results of load-settlement behavior and failure mechanism of both unreinforced and reinforced group is studied. The testing results indicated reduced lateral bulging and higher stone column load capacity for horizontally reinforced columns in comparison to vertically reinforced. For validation of experimental results, numerical modeling using finite element (FE) code Plaxis 2D has also been conducted. The FE results depict lower load capacity as compared to model testing for settlement of 30 mm. However, the failure mode for both model tests and FE analysis was marked by bulging near the top of stone column and

punching. Furthermore, load capacity is also check using empirical relations as given by IS code and previous literature. It is observed that experimental and analytical results are found in good agreement.

Keywords Stone column · Vertically reinforced · Horizontally reinforced · Geotextile · Plaxis 2D · Load carrying capacity · Bulging

1 Introduction

The construction of stone columns effectively reduces the settlement of the structure and the liquefaction potential of the soft surface by densifying the soil through vibrations and reinforcing the ground by the formation of a stiff composite soil mass. However, in extremely soft soils, the bulging out of the stone columns provides poor lateral confinement. This problem can be reduced to great extent by reinforcing the columns with highly stiff and creep resistant polymeric material commonly known as geosynthetic which offers sufficient lateral confinement pressure to the soil; thus avoids expansion of the column and helps in reduction of settlement of the structure. In view of this, stone columns can be encased vertically thereby resisting the bulging out by hoop stresses mobilisation in the geosynthetic (Fig. 1a) or the reinforcement can be horizontal (Fig. 1b), where the placing of geosynthetic discs at regular interval along the stone column

A. Thakur (✉) · S. Rawat · A. K. Gupta
Department of Civil Engineering, Jaypee University of
Information Technology, Solan, Himachal Pradesh, India
e-mail: ankit.thakur033@gmail.com

S. Rawat
e-mail: saurabh.rawat@juit.ac.in

A. K. Gupta
e-mail: ashok.gupta@juit.ac.in

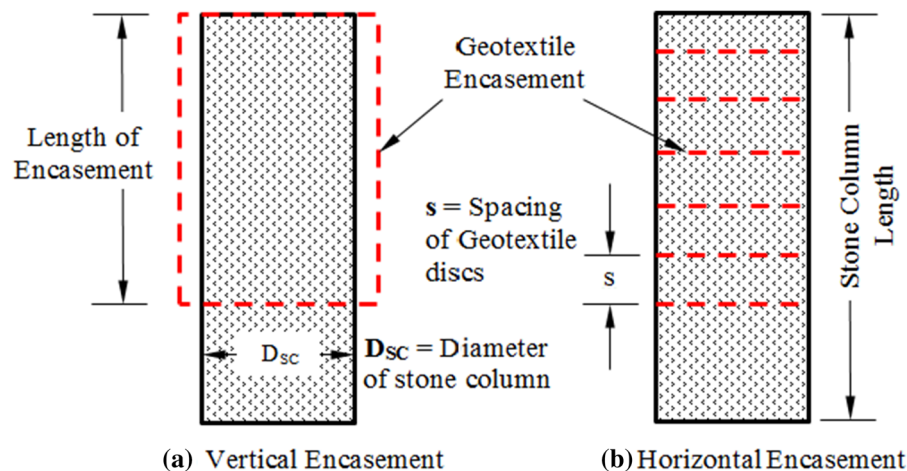


Fig. 1 Configuration of stone columns reinforcement

length provide mobilisation of frictional stress at the geosynthetic surface and expansion of the column can be avoided.

Among the pioneers with the idea of section encasement of stone columns, Van Impe and Silence (1986) carried out an investigation to survey the required geotextile quality. Similarly, Raithel and Kempfert (2000) and Pulko et al. (2011) studied the stone column settlement dependency on geotextile stiffness. Likewise, many researcher (Murugesan and Rajagopal 2006; Yoo and Kim 2009; Khabbazian et al. 2010; Lo et al. 2010; Zhang et al. 2012; Elsayw 2013; Almeida et al. 2013) have made number of numerical examinations on geosynthetic-encased stone columns primarily focussing on soft/weak cohesive soils. Malarvizhi and Ilamparuthi (2007) designed a number of consolidated programs of experimental testing and numerical modeling on completely encased, isolated sand columns by model footings to demonstrate the fundamental decrease in bulging of stone columns with expanding geogrid stiffness. Wu et al. (2009) also performed triaxial compression tests with various confining pressures on geotextile-encased sand columns by using three different types of geotextiles. The test results established that the reinforcement stimulates larger decrease in volumetric strain of the very loose specimen than that of the very dense specimen. Gniel and Bouazza (2010) investigated construction fragments of geogrids-encased stone columns. Sharma et al. (2004) conducted model tests to observe the bulging of horizontally reinforced stone columns and discovered that the bulging length in the reinforced

stone columns remained half as compared to unreinforced stone columns.

Murugesan and Rajagopal (2010) validated load tests on group of stone columns and confirmed that the load bearing capacity of geosynthetic-encased stone columns has expanded by 3–5 times with respect to unreinforced stone sections. They also examined that the performance of encasement is found to decrease with the diameter of the stone column. The experimental outcomes revealed the benefits of encasement on expanding the load bearing capacity of vertical encased stone columns (VESC). Gniel and Bouazza (2010) performed compression tests to inspect the efficacy of encasement construction using distinct geogrid and stone column aggregates. Sivakumar et al. (2004) compared the results of triaxial test series on sand columns models in clay with and without encasement. Wu and Hong (2009) presented a relationship for the prediction of axial stress–strain behaviour of granular stone columns and validated the relationship with results from triaxial test on reinforced sand specimen. The impact of encasement on granular stone columns by triaxial testing has also been studied by past researchers (Wu and Hong 2009; Gniel and Bouazza 2008) which reported that the increase in strength and firmness of granular stone columns is due to expanding confining pressure provided by reinforcement utilized. Hasheminezhad and Bahadori (2019) studied the seismic response of shallow foundations in liquefiable soils which was improved by deep mixing columns using a three dimensional finite model in FLAC. The results

revealed effective mitigation by artificially created non-liquefiable soil layer by the columns. The utility of soil–cement bed to improve bearing capacity and load carrying ability of stone columns has also been investigated by Das and Dey (2020a, b). Also, Dey and Debnath (2020) used empirical approach to estimate the bearing capacity of geogrid reinforced sand over vertically encased stone columns floating in soft clay using support vector regression. Hataf et al. (2020) studied the effect of length of encasement and the type of aggregate on the bearing efficiency of single column in both dry sand and clay bed using experimental and numerical approach. The findings of their study showed that reinforcement stiffness reduces with increase in the cohesion of the clay.

As per the literature review, vertically reinforced stone columns have been studied by many researchers primarily on soft cohesive soils. However, only few studies evaluating the behaviour of vertically reinforced columns in weak cohesionless soils are reported. Similarly, literature on reinforcement of stone column using horizontal discs of geosynthetics is virtually non-existent. Also, the review of literature reveals the efficacy of numerical modelling (Plaxis 2D and 3D) in thorough comprehension of reinforced stone column behaviour. Therefore, the current investigation deals with model tests on stone column reinforced composite ground using group of three and four stone columns in weak cohesionless soil. The stone columns of diameter 40 mm used in the present study are encased using geosynthetics both in vertical and horizontal direction. For comparison, testing has also been conducted for uncased stone column. An appraisal of relative increment in a load bearing capacity of the composite ground alongside by examining the mechanism of column failure in various cases are striking highlights of this investigation. The discoveries of the model tests on the ground improved with group of three and four stone columns are also validated by finite element method (FEM) using Plaxis 2D. Furthermore, validation of results has also been done against equations and formulation as given in concerned design IS codes and related published literature.

2 Materials Used

2.1 Soil and Aggregates Used

Most of the reported literature has been around improving the performance of soft cohesive soils using stone columns. Since existence of weak cohesionless soil up to a few metres of depth over a stiffer stratum is not uncommon in actual field condition, investigation of ground improvement techniques such as reinforced stone columns over traditionally available vibro-floatation or dynamic compaction methods should be assessed which is more economical and provides significant densification (Samanta et al. 2010). Therefore, evaluation of reinforced stone column performance in cohesionless soil (sand) is required for estimation of its load carrying potential, subsequent settlement and to develop design approach that can be used without detailed subsurface investigation. Moreover, as per FHWA (Barkdale and Bachus 1983), soil lying in the transition zone defined as the range of particles varying between 0.02 and 0.6 mm is found to response better to vibro-compaction than vibro-floatation. Since, installation of stone columns is carried out using compaction in the present study; it is highly recommended that the surrounding soil is sand. Moreover, for grain size distribution curve falling in the transition zone, the contact between the vibrator and host medium is improved significantly by using aggregate filled columns (Chenari et al. 2019). Hence for the above mentioned reasons, stone columns have been studied in sand. The soil used in the model tank was checked for particle size distribution, specific gravity, compaction properties and shear strength parameters. The laboratory testing for determination of soil properties were carried in accordance to the IS codes. The stiffness parameter (E) of the used soil was also determined from the shear load–displacement curve as given by Noonan and Nixon (1972). All the evaluated soil properties have been summarized in Table 1.

Construction of stone columns has been critically governed by the size of the aggregates used. The particle size (d) range of crushed aggregates/gravels used in field practice varies between 25 and 50 mm for construction of stone columns having diameter (D_{SC}) in range of 0.6–1.0 m. According to Ali et al. (2014), the crushed stones of size in between 6 and 40 mm can be chosen as aggregates depending upon the D_{SC}/d

Table 1 Tests and properties of the soil, aggregate and geotextile used

Test name	Parameter	Soil	Aggregates	Parameter	Encasement material
Sieve analysis	Soil name	Sand (SP)	Gravel (GP)	Material name	Geotextile
	D ₁₀	0.38	3.4	Stiffness	150 kN/m
	D ₃₀	0.55	4.0		
	D ₆₀	0.90	5.1	Tensile yield strength (N _p)	45 kN/m
	Coefficient of uniformity (C _u)	2.37	1.5		
	Coefficient of curvature (C _c)	0.89	0.92		
Direct shear test	Cohesion (<i>c</i>)	1.96 kN/m ²	0.10 kN/m ²	Mass per unit area	200 g/m ²
	Angle of internal friction (ϕ)	20°	43°		
Specific gravity test	Specific gravity	2.65	–		
IS compaction test	Optimum moisture content	8.40%	–	Axial stiffness (EA)	75,000 kN/m
	Saturated unit weight (γ_{sat})	21.75 kN/m ³	23.25 kN/m ³		
	Dry unit weight (γ_d)	15.7 kN/m ³	22.78 kN/m ³		
Direct shear test	Young's modulus (E)	20,000 kN/m ²	55,000 kN/m ²	Young's modulus (E)	150,000 kN/m ²
	Poisson's ratio (ν)	0.30	0.30	Poisson's ratio (ν)	0.35

ratio of 12–40 as used for prototypes (Ali et al. 2014; Wood et al. 2000). Thus, for the present study, with D_{SC}/d ratio of 4–20, size of aggregates varying between 2 and 10 mm were used for construction of model stone columns with $D_{SC} = 40$ mm. The aggregates were obtained from Hardik Construction Company, Panipat, India and evaluated for particle size distribution, dry density (Malarvizhi and Ilamparuthi 2007; Alexiew and Raithel 2015; Chen et al. 2015; Elshazly et al. 2008; Adam et al. 2010) and shear strength parameter using direct shear test conducted at a shearing rate of 1.25 mm/min under normal stress of 100 kPa, 150 kPa, 200 kPa and 300 kPa for determination of angle of internal friction of stone aggregates. The properties of aggregates determined from laboratory testing have also been given in Table 1.

2.2 Encasement Material: Geotextile

The use of stone column in weak cohesive soils is governed by the fact that failure of stone columns is marked by bulging which results in squeezing of aggregates into the surrounding soil. Additionally, use of stone columns in cohesive soils also facilitates rapid dissipation of excess pore water pressure by acting as

drainage path for the surrounding low permeable soil. Hence, with the primary aim of only increasing lateral confinement without hindering the drainage potential of stone columns, geogrids have been utilized for column confinement. However, use of geogrids for column confinement has been found to perform well for end-bearing columns as compared to floating columns. This based on the fact that if geogrid is used as a confining material for floating stone columns, settlement of columns occur prior to development of hoop stresses resorting to the high stiffness of geogrid (Ali et al. 2014). This is highly undesirable for case of floating columns. In case of geotextile used as confining material, hoop stresses are developed in the stone column and transferred laterally to the confining geotextile, thereby mobilizing the stiffness of the confining material and consequently bulging of stone columns. On further increasing the load, the geotextile reinforced stone column undergoes settlement. As per Ali et al. (2014), for floating stone columns with 30 mm diameter, geogrid-reinforced stone column depicted a load carrying capacity of 24% in comparison to 46% as obtained by geotextile-reinforced floating column. Similarly with increase in stone column diameter from 30 to 50 mm, geotextile

encased stone columns performed better with a load carrying capacity of 47% in comparison to 26% capacity rendered by geogrid encased floating column. For horizontally reinforced floating stone columns, equivalent load carrying capacity of 10% was observed for both geogrid and geotextile stone columns (Ali et al. 2014). Geogrid encased columns are found to perform better than geotextile encased columns in case of end-bearing columns as penetration of stone columns is restricted and hence mobilization of hoop stress occurs in the stiffer geogrid encasement. Thus, bulging is restricted and higher bearing capacity is obtained.

Since, the present study deals in with floating stone columns in sand (free-draining soil), dissipation of excess pore water pressure or in generally role of stone columns for providing a drainage blanket is unlikely to be critical. Moreover, prevention of lateral squeezing of aggregates into the surrounding sand for mobilization of hoop stresses and failure by bulging prior to settlement can precisely be attained by using geotextile (less stiffer than geogrid) as confining material.

The encasement material used was woven Polypropylene geotextile which can manage huge measure of burden with low permeability. The geotextile and its corresponding properties were obtained from SUNTECH Geotextile Pvt. Ltd., Chhattisgarh, India (Table 1). These geotextiles are also utilized in streets, runways, repositories and holding dividers. Also, for case of horizontal reinforcement in form of circular disc, the ease of obtaining a perfectly circular fabric (i.e. of diameter slightly smaller than the column diameter) is more convenient as compared to a much stiffer geogrid material. Hence, for the floating columns used in the present study only geotextile has been used.

3 Experimental Set-up

3.1 Model Tank Dimensioning, Scale Effect and Boundary Effect

The modeling of test tank and stone column parameters [diameter (d) and length (l)] are determined after considering the geometric similitude ratio, l/d ratio and boundary effects. For prototype stone columns, diameter range between 0.6 and 1.0 m with length of 5–20 m is generally used (Wood et al. 2000).

Moreover, the minimum diameter of stone column which can be installed with complete integrity is about 13 mm (Shahu and Reddy 2011). However, for the present study, diameter of stone column used is 40 mm rendering a similitude ratio ($d_{\text{model}}/d_{\text{prototype}}$) of 0.04–0.06. Similarly, l/d ratio used for prototypes varies from 5 to 20 (Shahu and Reddy 2011). Keeping in line with the mentioned norm, l/d ratio for the present study is maintained at 8. For dimensioning of the model tank, the most important parameter is that insignificant induced stresses are generated at the tank boundaries. This implies that the boundaries of the tank should be distant enough so that no constrained are developed and hence overestimation of results can be checked. In order to attain this, a hypothetical footing of width ($B = 120$ mm) resting on stone column of length (L) of 300 mm is considered. The adopted dimensions of $B = 120$ mm and $L = 300$ mm are considered for the maximum adopted model column dimensions. As adopted from the settlement concept of pile group, an equivalent footing is considered at two-third column length (i.e. at depth of 200 mm from ground). Using 2:1 dispersion method, the effect of vertical stress from footing resting on stone columns at the ground surface is calculated at depth of twice the footing width ($2B = 240$ mm below the equivalent footing location).

It is found that only 11% of stresses are developed at tank boundaries. However, considering the critical length for settlement criteria of $1.5 B$ (Wood et al. 2000; Ali et al. 2012), the vertical stresses developed due to footing surcharge are calculated at 180 mm below the location of hypothetical footing situated at 200 mm from ground level. It is found that only 16% of the total applied vertical stress is found at a depth of 380 mm from ground surface and it further reduces to 11% at a depth of 440 mm. Hence, considering any depth for model tank above 440 mm can be treated to be free from boundary effects. Similar approach for dimensioning of model cylindrical tank of diameter 300 mm and 600 mm-depth was also adopted by Shahu and Reddy (2011). On similar line, cylindrical model tanks for single and group of reinforced stone columns were also considered by Ali et al. (2012, 2014). In the present work, the depth of model tank taken is 550 mm, which applies that only 3% of the applied vertical stress reaches the tank boundaries.

However, for soft compressible soil, 16% of overburden stress can be significant, but that is only corresponding to the depth of 1.5 the footing width. The adopted depth in the present case is significantly higher (550 mm) depicting only 3% overburden stress which can be considered insignificant for soft compressible soils too. For considering the lateral boundaries, in addition to the 2:1 dispersion method, the concept of tributary area has also been taken into account. As per IS 15284 – 1 (BIS 2003), the tributary area (i.e. surrounding volume of soil) contributing to a stone column group arranged in triangular pattern is generally hexagonal and square for stone group column arranged in square pattern, respectively. The tributary area is transformed into a circle (cylinder) of the same cross-sectional area having an equivalent diameter of 1.05 times spacing between stone columns (s) for triangular arrangement and 1.13 s for square pattern (Castro 2017). Based on this, it is found that for the present triangular arrangement of stone columns of diameter 40 mm and spacing (s) of 120 mm, the equivalent unit cell diameter of 126 mm is obtained. This suggests that the each outermost stone column should be installed at a minimum distance of 63 mm from the tank boundaries. Similar for square arrangement, the minimum clear distance between centre of outermost stone column and lateral boundary should be at least 68 mm. In the present study, a clear distance between centre of outermost stone column and lateral tank boundaries is taken as 70 mm for all the model testing. Moreover, the lateral boundary distance of 70 mm also provides for development of complete pressure bulb formation $1.5 d = 60$ mm (Castro 2017), where $d =$ diameter of stone column = 40 mm primarily near the top of the stone column without any interference from the lateral boundaries.

Hence, it can be seen from Fig. 2 that induced stresses become insignificant at the adopted model tank dimensions of 300 mm (length) \times 300 mm (width) \times 550 (depth) mm with 3 sides made up of iron and 1 side of acrylic sheet.

3.2 Preparation of Sand Bed

Sand bed was prepared in model tank having the dimension 300 \times 300 \times 550 mm. The sand is filled using rainfall technique with each layer having thickness of 10 cm. The unit weight of each layer is kept constant for bulk density of 19.7 kN/m³, checked

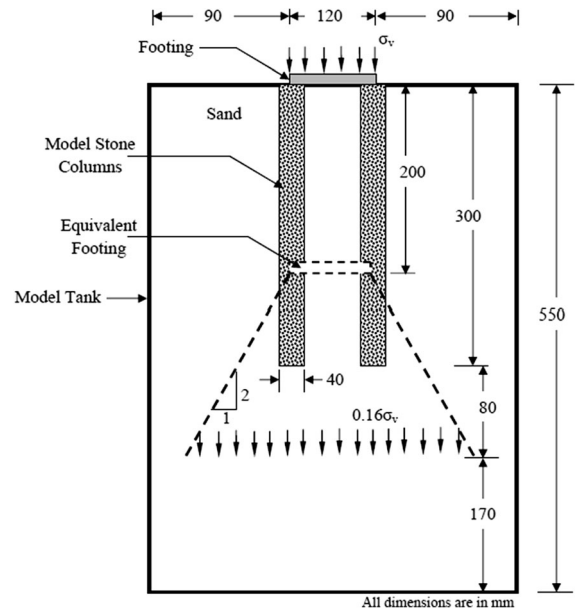


Fig. 2 Schematic view of model stone columns

continuously using a mould of known volume at three different locations within the layer during filling. Total 5 layers of sand are made and final attainment 50 cm height is achieved. The inner faces of the walls of the model tanks were coated with the layer of grease in order to reduce the friction between the model tank and the sand. A tracer in the form of a red and yellow powder dye is also used for marking after every 10 mm layer so as to identify the deformation patterns developed during stone column testing. The top surface of the sand bed was levelled and cut to have a genuine thickness and surface in all tests. A similar technique was utilized in all tests for the preparation of the sand bed. For all sand layers, the water content profile was resolved at 10 cm interims to guarantee that constant moisture content maintained throughout the model tank.

3.3 Construction and Installation of Stone Columns

In all tests (unreinforced/uncased and reinforced/encased), stone columns with diameter of 40 mm for group of 3 and 4 stone columns were constructed. The stone column parameters [diameter (d) and length (l)] are determined after considering the geometric similitude ratio, l/d ratio and boundary effects. For prototype stone columns, diameter range between 0.6 and

1.0 m with length of 5–20 m is generally used (Wood et al. 2000). Moreover, the minimum diameter of stone column which can be installed with complete integrity is about 13 mm (Shahu and Reddy 2011). However, for the present study, diameter of stone column used is 40 mm rendering a similitude ratio ($d_{\text{model}}/d_{\text{prototype}}$) of 0.04–0.06. Similarly, l/d ratio used for prototypes varies from 5 to 20 (Shahu and Reddy 2011). Keeping in line with the mentioned norm, l/d ratio for the present study is maintained at 8.

The group of stone columns used in practice are uniformly distributed in triangular or square pattern. Due to this orientation, each column of the stone column group projects a tributary area to the surrounding soil which is in form of a hexagon for triangular grid and square for square grid, respectively. Thus, for easy of theoretical analysis and converting the problem to an axi-symmetric condition, the tributary areas is transformed into circles (cylinder in 3D) of equivalent cross-sectional area. Hence, for triangular shape, the equivalent diameter of the corresponding unit cell is equal to 1.05 times the column spacing 's' and 1.13 s for square shaped group distribution (Castro 2017).

The casting of stone column has been done using the soil replacement technique. This technique has been employed by other researchers in the past (Black et al. 2011; Mohanty and Samanta 2015) for small-scale stone column installation in comparison to soil displacement, frozen and force intrusion techniques. For casting of stone columns, a PVC casing of internal diameter 40 mm and thickness of 2 mm was used. Using a hydraulic jack, the PVC casing was inserted into the sandy soil. The main reason for using the top down techniques was to avoid the caving of soil during borehole formation. The soil within the PVC casing was removed using a screw type auger of 38 mm diameter. The remaining soil was scooped out from inside the casing. Prior to placing of aggregates, the interior walls of the casing were greased so as to avoid wall friction and facilitate easy retrieval of casing. The IS light compaction hammer weighing 2.6 kg was used to compact the stone aggregates. The height of fall and number of blows was determined through trial and error prior to casting for a 100 mm stone aggregate thickness so that a desired relative density of 65% ($\gamma_d \approx 23 \text{ kN/m}^3$) is attained. The high relative density of 65% is attributed for attaining efficient load transfer (strength) over its drainage facility as the

surrounding soil itself is permeable by nature. However, in the reported literature (Black et al. 2011; Mohanty and Samanta 2015), relative densities of 50–80% have been used for stone column in clayey soil domain. The aggregates are placed within the casing and tamped while the casing is retrieved simultaneously. Care is taken that only 80 mm of casing is retrieved after laying of each layer so that a seating of 20 mm is available for placement of following stone aggregate layer. The variation of relative density was assumed to be $65 \pm 2\%$ during aggregate placement. However, the %age variation in relative density of casted columns with horizontal reinforcement was assumed to be higher as precise compaction of stone layer thickness of only 30 mm was difficult to execute (Fig. 3).

Similarly, installation of vertically encased/reinforced stone columns consisted of attaching the geotextile encasement outside the casing pipe. It is realized that the deformation in stone columns in the form of bulging under loading occurs up to a depth of 1.5–2 times the stone column diameter measured from the top of the stone column. Thus, lateral confinement of the top depth of stone column becomes critical to diminish the bulging. Murugesan and Rajagopal (2006) conducted numerical investigation on stone column encasement and reported that beyond a depth equal to double the column diameter does not contribute to capacity improvement. Consequently, the confinement of only the top portion of the stone columns has been adopted for the present research. In order to better comprehend the reinforcing behaviour, a few tests were also performed on with encasement of full length of stone columns. As mentioned above, the geotextile + casing set-up is embedded during the laying of progressive layers. For ease of retrieval, the external surface of the casing is properly greased. The aggregates are gradually filled inside the casing along with tamping. With the withdrawal of casing, a stone column consisting of geotextile packed with aggregates is obtained.

In development of horizontal reinforced stone columns, disc shaped geotextiles having diameter of 40 mm are placed at spacing of 30 mm throughout the length. For horizontally reinforced columns the diameter of reinforcement (circular discs) was indeed slightly smaller (39.5 mm) than the column diameter of 40 mm. However, the value was rounded off to 40 mm when stated in the manuscript. The authors

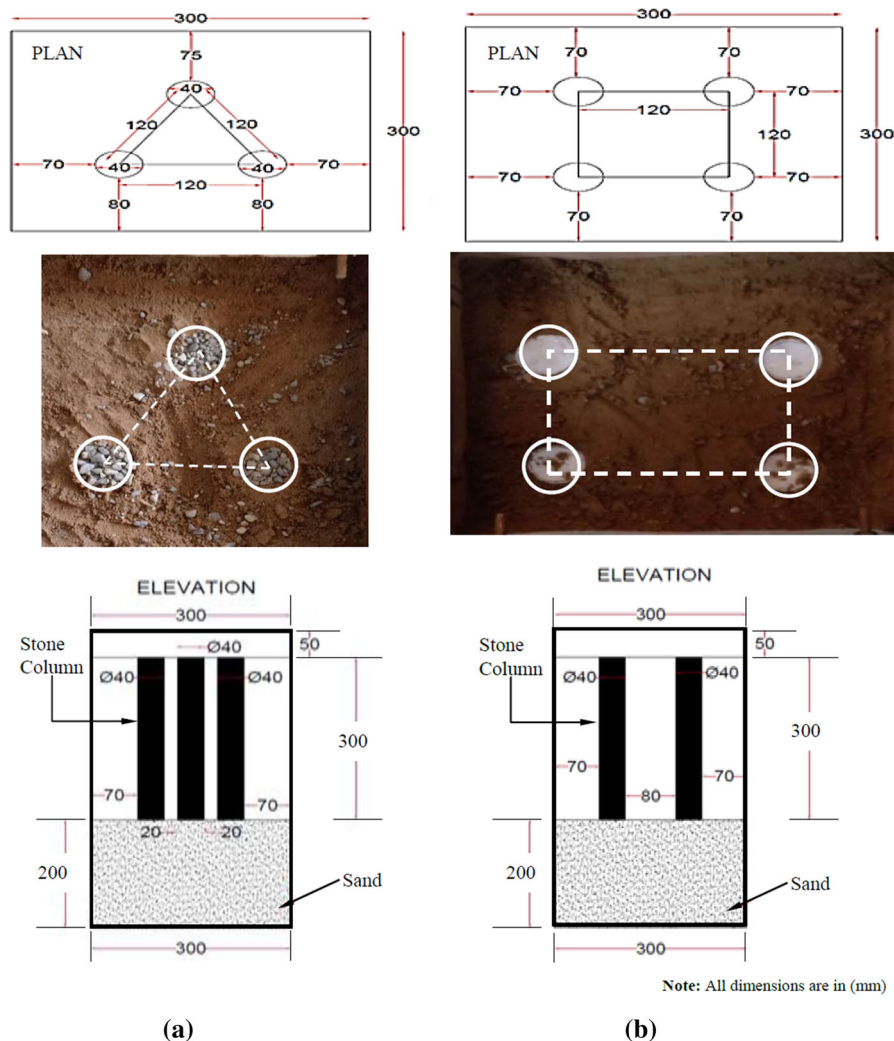


Fig. 3 View of stone columns in plan and elevation for **a** 3—stone columns, **b** 4—stone columns

have incorporated the actual value in the revised manuscript as per the suggestion. Ali et al. (2014) reported that maximum increase in failure stress is attained for horizontal reinforcement spacing of $d/2$ (where d is the diameter of the stone column) or $s/d = 0.5$ (where ' s ' is the spacing between the reinforcement). Likewise, the horizontal spacing of reinforcement for the present work should have been 2 cm for column dia. of 40 mm. However, the failure stress is also found to vary with increasing x/l ratio from 0.5 to 1.0, where ' x ' = distance of horizontal reinforcement from top of stone column and ' l ' is column length. The failure stress is found to increase from 18% for $x/l = 0.5$ to 25% for $x/l = 1$. Thus, to assess the variation of x/l ratio and s/d criteria, the

present work adopts spacing at 3 cm. This enables evaluation of x/l ratio from 0.1 to 0.9 and s/d ratio of 0.75. The casing pipe was marked at 30 mm spacing, in order to facilitate accurate positioning of horizontal encasement. As the aggregates are filled and tamped, circular discs are placed at each marking with the help of the tamping rod. Alternatively, casing pipe is withdrawn gradually. In the current research 3 different tests were performed for each 3 stone columns and for 4 stone columns namely for unreinforced stone columns, encased stone columns and horizontally reinforced stone columns.

3.4 Testing Procedure

In practice, loading of stone columns is carried out with an area replacement ratio (A_r) varying between 10 and 35% (Mohanty and Samanta 2015). In the present study, uniform load is applied on the group of 3 and 4 stone columns using a square plate of dimensions 200×200 mm and thickness of 10 mm. The thickness of the loading plate was determined after trial and error method, so that negligible plate deformation occurs under loading. The dimensions of the plate was determined such that the $A_r = 18\%$ for group of 3 stone columns and $A_r = 26\%$ for group of 4 stone columns. The A_r so adopted is in accordance to Ali et al. (2014) where a constant A_r equal to 25% was adopted. The load was then applied using a modified plunger of diameter 80 mm so that for a unit cell the tank dimensions are 3–5 times the diameter of the loaded area. The plunger was attached to the UTM machine and compressive load at a rate of 1kN/min was applied. The load application was ceased when settlement of stone column group reached 30 mm. The control unit of UTM provided real time recording of both the applied load and corresponding vertical displacement of the stone columns (Fig. 4).

This vertical displacement is indicative of the stone column settlement. The difficulty in evaluating the results is the prediction of load carried and settlement undergone by each column. Moreover, quantification of bulging suffered by each column can only be evaluated through exhumation. The present investigation includes applied vertical stress measured in terms

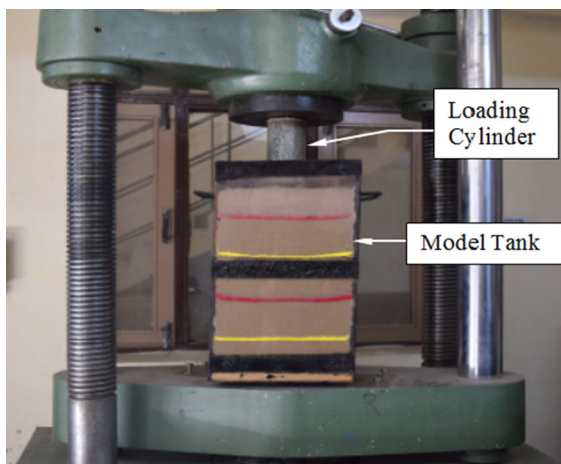


Fig. 4 Complete model set—up in the loading machine

of footing pressure which was calculated as ratio of total load by area of the footing.

Since increase in bearing capacity obtained from vertically encased and horizontally reinforced stone columns is almost equivalent, a combined vertical and horizontal reinforcement was not studied in the present work. Moreover, field studies regarding combined vertical and horizontal reinforcement are virtually non-existence. Hence, investigation of stone column reinforced both vertically and horizontally can be taken up by future researchers through small scale or field scale testing. Similarly, more sophisticated instrumentation is required for evaluation of load capacity and settlement of individual reinforced and unreinforced columns. For quantifying the bulging and further assessing the reinforcing action in vertical and horizontal stone column reinforcement, strains developed along the stone columns should be recorded and analyzed. Similarly assessment of variation of earth pressure around the stone columns can provide significant insights in view of the mode of failure suffered by respective reinforced stone columns. However, all the above mentioned observations are beyond the scope of the present work.

3.5 Numerical Modelling using Finite Element Method (Plaxis 2D)

The state of stress around the stone column (unreinforced and reinforced) is generally non-linear in nature. However, use of the concept of unit cell, stone columns can be studied numerically using axisymmetrical model (Castro 2017). The soil around the stone columns is modelled as elastic–plastic using the Mohr–Coloumb soil model. The simulation of soil has been carried out using soil properties as given in Table 1. The simulation of used soil in Plaxis 2D requires values of c , ϕ , γ_{bulk} , γ_{sat} , E and ν . To accurately model the boundary conditions of the model tank, bottom of the model were restricted in x , y and z directions. However, for allowing stone column settlement under loading, vertical boundaries were not restricted in the z -direction. Ambly and Gandhi (2007) conducted the analysis of unreinforced stone columns without interface element and reported the deformation of column mainly due to radial bulging and there occurred no significant shear. The interface between the stone columns and soil depends upon the method of installation and its shear properties can vary

significantly. Therefore, in the present study of unreinforced columns, no interface zone was used.

For modelling of reinforced stone columns, geotextile encasement was modelled using geogrid element as provided by Plaxis code. This element modelled as an ‘elastic’ material requires the use of axial stiffness (EA) for simulating the material stiffness where ‘E’ is the Modulus of elasticity of geotextile and ‘A’ is cross-sectional area of geotextile (Table 1). The efficacy of the modelled reinforced stone columns is governed by the modelling of the interface between the soil and encasement material. Plaxis 2D allows the use of an interface reduction ratio (R_{inter}) for precise modelling of the interfaces (Brinkgreve et al. 2010). The value of R_{inter} reflects the mobilization of interface friction ($\tan\delta$) with respect to the angle of internal friction of soil ($\tan\phi$). For the present analysis, interface reduction value ($R_{inter} = 1.554 \approx 1.0$) as obtained from direct shear test is used for modelling the interface friction between geotextile and soil interface (Fig. 5).

The complete models were meshed in two-dimensional environment with fine meshing around the stone columns and gradually coarser in the radial direction. The discretization of soil and stone columns has been carried out using 15-noded triangular elements. Prior applying the load, in-situ stresses were generated using the K_0 -procedure through Jacky’s formula of $1 - \sin\phi$. The loading of stone columns has been applied in the form of vertically pre-described displacement and analyzed using plastic calculation which evaluates failure load at various displacements values till the pre-described displacement is ultimately reached. The limitation of the present FE modelling lies in the fact that lab installation procedure of stone columns is not taken into consideration and stone columns are modelled as embedded elements.

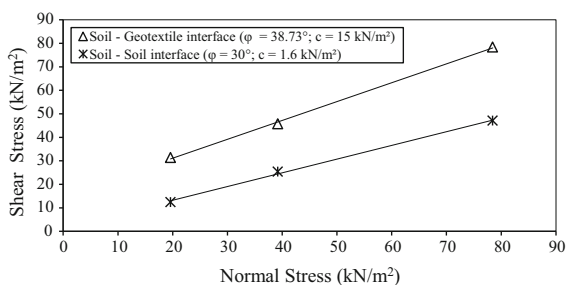


Fig. 5 Interface shear strength

4 Results and Discussions

4.1 Failure Mechanism of Group of Stone Columns: Model Testing

The failure of the group columns is considered at a displacement of 30 mm. The set-up was removed from the loading machine and the stone columns were exhumed. The deformed shapes of groups of uncased stone columns were analysed. It was seen that the failure is accomplished by bulging of stone columns. The bulging failure occurred at a distance of D to $2D$ from the top of the stone columns for both groups of uncased 3 and 4 stone columns. In addition to the bulging failure, lateral deflection of the uncased stone columns is also observed. The lateral displacement of stone columns was generally in inward direction. The lateral deformation that is produced during present testing was similar to that of the lateral deformation observed by the Wood et al. (2000). The inward lateral displacement of group of uncased stone columns is attributed to the stresses mobilized within the stone columns under loading.

As the vertical stress is transferred uniformly to all the stone columns, hoop stresses develop within the stone column. This results in lateral bulging of stone column. Since the stone columns are encased in a material having significant tensile strength, stone columns are able to withstand large magnitude of hoop stresses (Fig. 6). The testing results revealed that bulging and lateral deformation was found to be less for all reinforced stone columns as compared to unreinforced stone columns. Since the bulging occurs only at the top $2D$ of stone column, it signifies that soil stresses around this depth are less as compared to the bottom of stone column. Thus the stone column base behaves like a fixed end, resulting in the inwards lateral deflection of the stone columns.

4.2 Failure Mechanism of Group of Stone Columns: Plaxis 2D

Figure 7a, b show the deformed shapes for 3 and 4 stone columns after loading. As observed in group of 3 stone columns as shown in Fig. 7a, the causes of deformation are because of bulging and also due to lateral deformation. However in the case of 4 stone columns Fig. 7b, the causes of deformation are because of bulging and also due to lateral deformation



Fig. 6 Exhumed vertically encased stone columns after group testing **a** 3 stone columns, **b** 4 stone columns

in the periphery of the stone columns. The lateral deformation of the columns can be diminished by using vertical reinforcement because there is no bending stiffness in this type of reinforcement.

4.3 Load-Settlement Behaviour: Model Testing

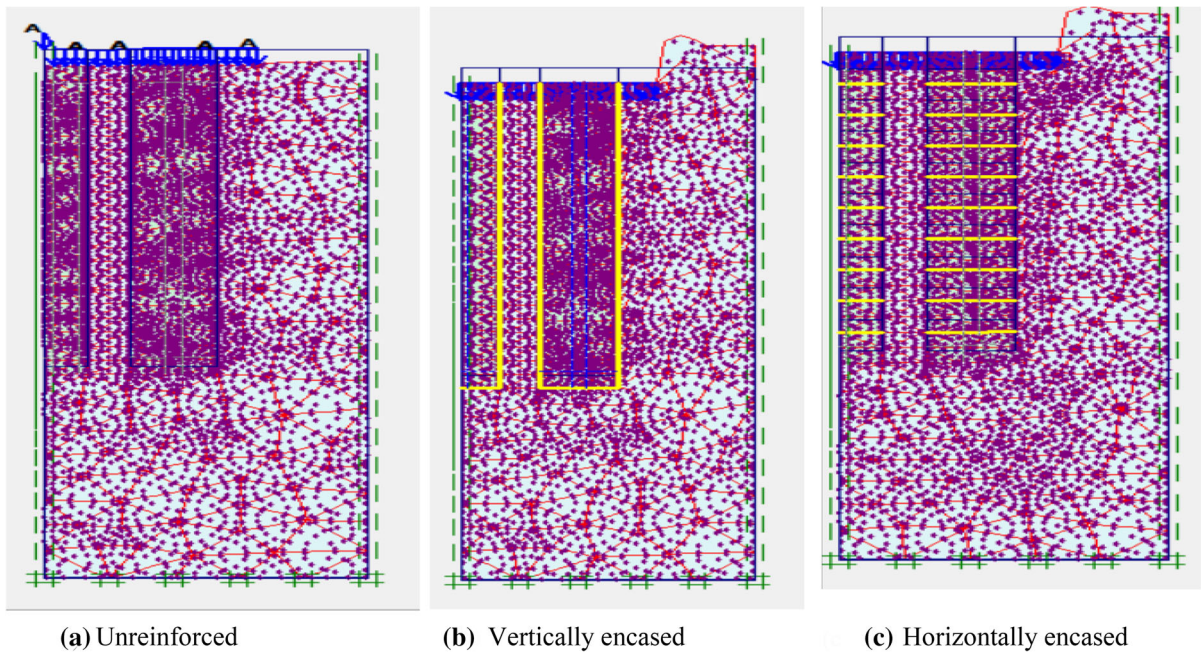
The load settlement behaviour for 3 and 4 isolated stone columns with diameter 40 mm has been illustrated in Fig. 8a, b. It has been seen that the load carrying capacity of the weak soil gets increase after the implication of the stone columns. Unreinforced stone columns start failing at lower load in comparison with the reinforced one. This is because when geotextiles are applied as vertical and horizontal reinforcing material to the stone columns, the lateral squeezing of aggregates into the surrounding soil is restricted due to encasement in case of vertically reinforced stone columns and increases shearing resistance against bulging for horizontally reinforced floating stone columns. From Fig. 8a, b, it is obvious that horizontal reinforcement provides greater load bearing capacity due to restricted bulging as a consequence of increased shearing resistance developed at the aggregate-geotextile disc-aggregate interface.

As shown in Fig. 8a, b, the reason for load-settlement behaviour to start from nil vertical deformation can be attributed to the mobilization of hoop stresses in the confining material. The failure mechanism of confined stone columns is generally marked by development of hoop stresses in the stone column as the footing load increases gradually. In absence of encasement material, the generated hoop stresses are

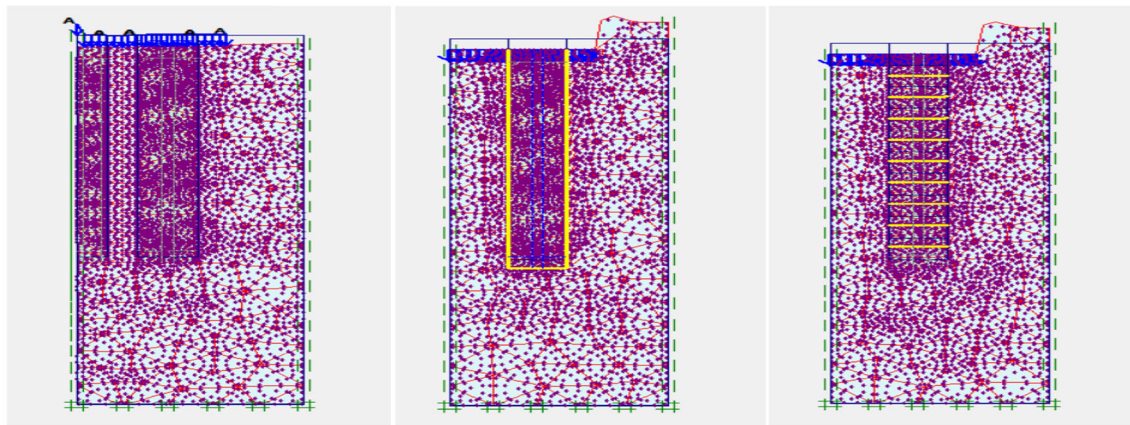
transferred into the surrounding soil leading to bulging and consequent failure. In case of encasement is available, the developed hoop stresses are transferred to the geotextile material which undergoes laterally deformation (limited bulging). On further increasing the footing load the hoop stresses are transferred to the bottom of the encased stone column which results in the penetration of stone column (settlement). Therefore, during experimental testing, initially as hoop stresses are transferred to the geotextile encasement, nil deformation is observed. Now as the load is increased further, hoop stresses are transferred to the bottom of the stone column which results in the settlement of stone columns. In addition to this, nil displacement with initial loading can also be due to the applied seating load prior to testing for development of equilibrium in-situ stresses.

4.4 Load-Settlement Behaviour: Plaxis 2D

It can be seen from Fig. 9a, b that similar to model testing the stone column are found to depict more load carrying capacity for horizontally reinforced stone columns than unreinforced. The results are consistent for group of 4 stone columns. However, it is observed that load carrying capacity for unreinforced and reinforced stone columns are found to be more as compared to the experimental values. This increase can be attributed to the simulation of stiffer soil-geotextile interface and boundary conditions. Also the limitation of modelling stone columns without installation effects fails to simulate the remoulded properties of soil which occurs during model testing. This leaves the soil to behave with undisturbed shear



(a) Deformed mesh for group of 3 stone columns

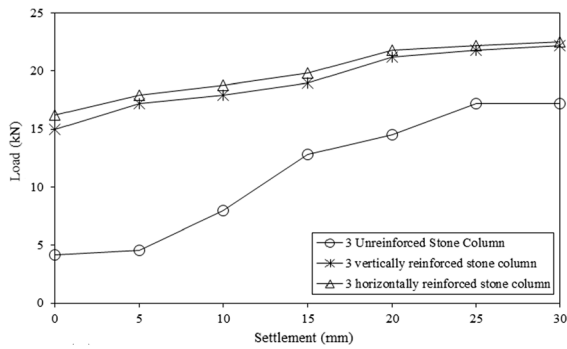


(b) Deformed mesh for group of 4 stone columns

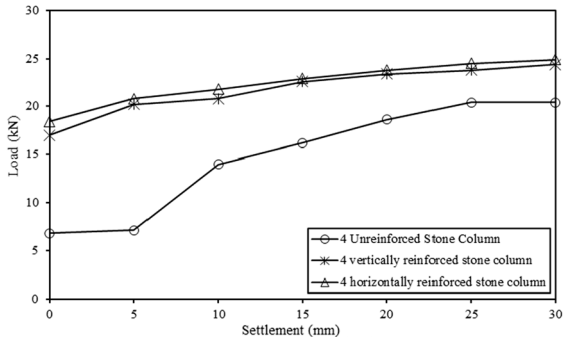
Fig. 7 **a** Deformed mesh for group of 3 stone columns. **b** Deformed mesh for group of 4 stone columns

strength values in contrast to remoulded shear strength which governs the stone column behaviour during testing. It is observed that the percentage increase between FE predicted and experimental load carrying capacity is between 30 and 40% for all the cases of 3 and 4-stone column group (Table 2). However, for 4-stone column unreinforced group, percentage increase of only 22% is obtained.

Another striking observation with regard to the FE results is the gradual settlement of stone columns obtained with loading. This behaviour is in contrast to the experimental curves (Fig. 8a, b) and can be related to the rough nature of modelled interface. The maximum default (R_{inter}) as used by Plaxis 2D can only be 1.0. This models a rough aggregate–geotextile interface and geotextile–sand interface which results in a high interface stiffness as compared to the less stiff



(a) Load – settlement variation for group of 3 stone columns



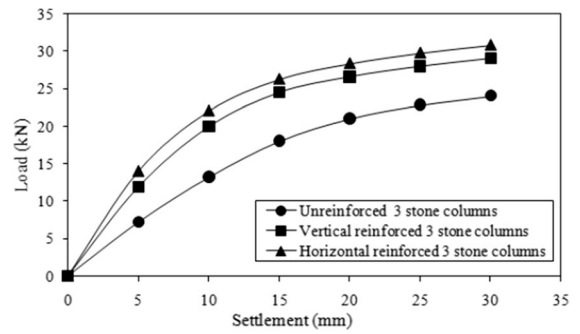
(b) Load – settlement variation for group of 4 stone columns

Fig. 8 a Load—settlement variation for group of 3 stone columns. b Load—settlement variation for group of 4 stone columns

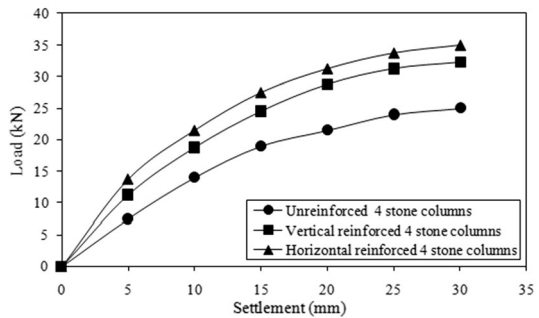
interface prevalent during model testing. Hence, in FE analysis hoop stresses developed under loading are directly transferred to the bottom of stone column on encountering the simulated stiffer interface and thus settlement is observed with loading. This shortcoming of simulation in Plaxis 2D is due to the limitation of precisely modelling of interface ($R_{inter} = 1$). Therefore, this trend is also consistent for all unreinforced and reinforced stone columns.

5 Validation of Results

For validation of the experimental results, a comparison has also been carried out using equations given by IS 15284 Part 1 (BIS 2003) for unreinforced stone columns. Likewise, for validating the load carrying capacity of reinforced stone columns, empirical relations as given by Murugesan and Rajagopal (2010) are also used. The load carrying capacity of the reinforced stone columns has been calculated theoretically using



(a) Load – Settlement variation for group of 3 stone columns from Plaxis 2D



(b) Load – Settlement variation for group of 4 stone columns from Plaxis 2D

Fig. 9 a Load—Settlement variation for group of 3 stone columns from Plaxis 2D. b Load—Settlement variation for group of 4 stone columns from Plaxis 2D

following equations (Murugesan and Rajagopal 2010; BIS 2003):

$$\sigma_v = (\sigma_{r0} + 4c_u)Kp_{col} \tag{1}$$

where σ_v is the maximum footing pressure acting on unreinforced stone columns, σ_0 represents the initial effective radial stress calculated as $2[1 - \sin(\varphi_{soil})]\gamma d$. For the present case, $c_u = 0$ and $Kp_{col} = \tan^2(45 + \phi/2)$ where ϕ is the internal frictional angle of the stone aggregates = 43° .

The value of σ_v can be used to calculate load on unreinforced group of stone columns (P) in kN is calculated by Eq. (2) as:

$$P = \sigma_v \times A \tag{2}$$

where A = Area of the unit cell given by $\pi \times (0.525 s)^2$ for triangular arrangement (3 stone column group) and $\pi \times (0.564 s)^2$ for square arrangement (4 stone column group) (BIS 2003) with

Table 2 Comparison of experimental and theoretical bearing capacities of unreinforced and reinforced stone column groups

Stone column arrangement	Reinforcement orientation	Model Testing Load capacity (kN)	FE analysis Load Capacity (kN)	Theoretical Load capacity from using Equation given by IS 15284 Part1 [1] and Murugesan and Rajagopal [2] (kN)	Final Settlement (mm)	Coefficient of Variance (COV) (%)
Triangular Arrangement [3 – stone column]	Unreinforced	17.2	24	22.2	30	16.67
	Vertically	22.2	29.05	17.31	30	25.80
	Horizontally	22.5	30.8	–	30	–
Rectangular Arrangement [4 – stone column]	Unreinforced	20.4	25	23.4	30	16.67
	Vertically	24.4	32.25	19.73	30	25.80
	Horizontally	24.9	35	–	30	–

s = spacing between the stone columns. The theoretical bearing capacity as obtained from Eqs. (1) and (2) are tabulated in Table 2.

For the evaluation of bearing capacity of vertically reinforced stone column groups, the design guidelines by Murugesan and Rajagopal (2010) have been followed where the area replacement ratio (A_r) has calculated using Eqs. (3) and (4):

For group of three stone columns:

$$A_r = 0.907 \left(\frac{d}{s} \right)^2 \quad (3)$$

For group of four stone columns:

$$A_r = 0.786 \left(\frac{d}{s} \right)^2 \quad (4)$$

here ‘d’ is the diameter of the column and ‘s’ is the spacing between the columns. Using the values of A_r corresponding values of normalized tension [$T/(d \times \sigma_v)$] in the stone column encasement has been obtained from the design chart by Murugesan and Rajagopal (2010). With tensile strength of geotextile (T) for the present case = 45 kN/m and ‘d’ = 0.04 m, σ_v for group of three and four stone columns has been evaluated. Thus, from Eq. (2), load on group of vertically reinforced stone columns has been determined and listed in Table 2. However, for horizontally reinforced stone columns, there is currently no

empirical relationship. It can also be seen from Table 2 that load carrying capacity as obtained from model testing, FE analysis and empirical formulation are found in good agreement with a maximum coefficient of variance of 25%.

6 Conclusions

In this present work, a number of experimental tests have been performed on group of 3 and 4 stone columns having diameter of 40 mm. Tests were carried for both unreinforced and reinforced stone columns i.e. by encasing the stone columns and by providing horizontal reinforcement to the columns. The results obtained from experimental testing were validated through finite element modelling using Plaxis 2D. Also, validation of load carrying capacity has been validated using the design formula as per IS code and published literature. Based on the results obtained, following conclusions have been made:

1. Geotextile reinforcement provides mobilization of higher hoop stresses than unreinforced stone columns, and thus better load carrying capacity at same settlement. Moreover, horizontal reinforcement increases the shearing resistance between the aggregate–geotextile–aggregate during bulging and hence renders better load capacity

in comparison to vertically encased floating columns.

2. The failure of reinforced stone columns is also marked by bulging primarily occurring at depth equal to the stone column diameter to twice the column diameter. Additionally, punching of stone column is observed for both unreinforced and reinforced stone columns. Similar failure mechanism is also obtained from FE analysis.
3. The load-settlement behaviour of reinforced stone columns is governed by the stiffness provided by the encasement material. The difference between the load-settlement characteristics as obtained from model testing and FE analysis, it can be inferred that higher the stiffness of the encasement/confining material, lesser will be the bulging but consequently more settlement of floating stone columns.
4. For precisely modelling the stone column behaviour in finite element, the procedure of installation of stone columns is recommended. However, the FE renders similar failure mode but depicts higher load carrying capacity as compared to experimental values.
5. The load carrying capacity for reinforced 3 and 4 stone column groups are found in good agreement with FE results. Also, the model testing results are in accordance to the design formulas as given by IS 15284 Part1 [1] for unreinforced stone columns and empirical relations given by Murugesan and Rajagopal [2] for vertically reinforced stone columns. The results are within a maximum variance of 25%.
6. In absence of empirical relations regarding horizontally reinforced stone columns in published literature, it is recommended that based on field studies and more detailed model testing results, such relations are developed by future researchers.

Compliance with Ethical Standards

Conflict of interest On behalf of all authors, the corresponding author states that there is no conflict of interest.

References

Adam D, Schweiger HF, Markiewicz R, Knabe T (2010) Euro 2008 Stadium Klagenfurt–Prediction, Monitoring and back calculation of settlement behavior. In: Proceedings of the

From Research to Design in European Practice, Bratislava, Slovak Republic

- Alexiew D, Raithel M (2015) Geotextile-encased columns: case studies over twenty years. Embankments with special reference to consolidation and other physical methods. Butterworth-Heinemann, Oxford, pp 451–477
- Ali K, Shahu JT, Sharma KG (2012) Model tests on geosynthetic-reinforced stone columns: a comparative study. *Geosynth Int* 19(4):292–305
- Ali K, Shahu JT, Sharma KG (2014) Model tests on single and groups of stone columns with different geosynthetic reinforcement arrangement. *Geosynth Int* 21(2):103–118
- Almeida MSS, Hosseinpour I, Riccio M (2013) Performance of a geosynthetic encased column (GEC) in soft ground: numerical and analytical studies. *Geosynth Int* 20(4):252–262
- Ambily AP, Gandhi SR (2007) Behavior of stone columns based on experimental and FEM analysis. *J Geotech Geoenviron Eng* 133:405–415
- Barkdale RD, Bachus RC (1983) Design and construction of stone columns. Report No. FHWA/RD-83/02C, vol 1, Federal Highway Administration, Washington, DC
- BIS IS 15284-1: 2003. Design and construction for ground improvement - Guidelines - Part 1: Stone Columns, Bureau of Indian Standards, ManakBhavan, 9 Bahadur Shah ZafarMarg, New Delhi, India
- Black JA, Sivakumar V, Bell A (2011) The settlement performance of stone column foundations. *Geotechnique* 61(11):909–922
- Brinkgreve RBJ, Swolfs WM, Engin E, Waterman D, Chesaru A, Bonnier PG, Galavi V (2010) PLAXIS 2D 2010 User manual, Plaxisbv
- Castro J (2017) Modeling stone columns. *Materials* 10(7):782
- Chen JF, Li LY, Xue JF, Feng SZ (2015) Failure mechanism of geosynthetic-encased stone columns in soft soils under embankment. *Geotext Geomembr* 43:424–431
- Chenari RJ, Fard MK, Chenari MJ (2019) Physical and numerical modeling of stone column behavior in loose sand. *Int J Civ Eng* 17:231–244
- Das M, Dey AK (2020a) Use of soil cement bed in improvement of load carrying capacity of stone columns. *Geotech Geol Eng* 38:6529–6550
- Das M, Dey AK (2020b) Use of soil-cement bed to improve bearing capacity of stone columns. *Int J Geomech* 20(6):06020008
- Dey AK, Debnath P (2020) Empirical approach for bearing capacity prediction of geogrid-reinforced sand over vertically encased stone columns floating in soft clay using support vector regression. *Neural Comput Appl* 32(10):6055–6074
- Elsawy MBD (2013) Behaviour of soft ground improved by conventional and geogrid-encased stone columns, based on FEM study. *Geosynth Int* 20(4):276–285
- Elshazly H, Elkasabgy M, Elleboudy A (2008) Effect of inter-column spacing on soil stresses due to vibro-installed stone columns: interesting findings. *Geotech Geol Eng* 26:225–236
- Gniel J, Bouazza A (2008) Improvement of soft soils using geogrid encased stone columns. *Geotext Geomembr* 27(3):167–175

- Gniel J, Bouazza A (2010) Construction of geogrid encased stone columns: a new proposal based on laboratory testing. *Geotext Geomembr* 28:108–118
- Hasheminezhad A, Bahadori H (2019) Seismic response of shallow foundations over liquefiable soils improved by deep soil mixing columns. *Comput Geotech* 110:251–273
- Hataf N, Nabipour N, Sadr A (2020) Experimental and numerical study on the bearing capacity of encased stone columns. *Int J Geo-Eng* 11:1–19
- Khabbazian M, Kaliakin VN, Meehan CL (2010) Numerical study of the effect of geosynthetic encasement on the behaviour of granular columns. *Geosynth Int* 17(3):132–142
- Lo SR, Zhang R, Mak J (2010) Geosynthetic-encased stone columns in soft clay: a numerical study. *Geotext Geomembr* 28(3):292–302
- Malarvizhi SN, Ilamparuthi K (2007) Comparative study on the behaviour of encased stone column and conventional stone column. *Soils Found* 47(5):873–885
- Mohanty P, Samanta M (2015) Experimental and numerical studies on response of the stone column in layered soil. *Int J Geosynth Ground Eng* 1(3):27
- Murugesan S, Rajagopal K (2006) Geosynthetic-encased stone columns: numerical evaluation. *Geotext Geomembr* 24:349–358
- Murugesan S, Rajagopal K (2010) Studies on the behavior of single and group of geosynthetic encased stone columns. *J Geotech Geoenviron Eng, ASCE* 136(1):129–139
- Noonan DKJ, Nixon JF (1972) The determination of Young's modulus from the direct shear test. *Can Geotech J* 9(4):504–507
- Pulko B, Majes B, Logar J (2011) Geosynthetic-encased stone columns: analytical calculation model. *Geotext Geomembr* 29:29–39
- Raithel M, Kempfert HG (2000) Calculation models for dam foundations with geotextile sand columns. In: *Proceedings of International Conference on Geotechnical and Geological Engineering, GeoEng 2000*, Melbourne, Australia
- Samanta M, Sawant VA, Ramasamy G (2010) Ground improvement using displacement type sand piles. In: *Proceedings of the Indian geotechnical conference*, Mumbai, India, pp 629–632
- Shahu JT, Reddy YR (2011) Clayey soil reinforced with stone column group: model tests and analyses. *J Geotech Geoenviron Eng* 137(12):1265–1274
- Sharma RS, Kumar BRP, Ngendra G (2004) Compressive load response of granular piles reinforced with geogrids. *Can Geotech J* 41(1):187–192
- Sivakumar V, McKelvey D, Graham J, Hughes D (2004) Tri-axial test on model sand columns in clay. *Can Geotech J* 41:299–312
- Van Impe W, Silence P (1986) Improving of bearing capacity of weak hydraulic fills by means of geotextiles. In: *Proceedings of the 3rd international conference on geotextiles*, Vienna, Austria, pp 1411–1416
- Wood DM, Hu W, Nash DFT (2000) Group effects in stone column foundations: model tests. *Geotechnique* 50(6):689–698
- Wu CS, Hong YS (2009) Laboratory tests on geosynthetic encapsulated sand columns. *Geotext Geomembr* 27(2):107–120
- Wu CS, Hong YS, Lin HC (2009) Axial stress–strain relation of encapsulated granular column. *Comput Geotech* 36:226–240
- Yoo C, Kim SB (2009) Numerical modeling of geosynthetic-encased stone column-reinforced ground. *Geosynth Int* 16(3):116–126
- Zhang Y, Chan D, Wang Y (2012) Consolidation of composite foundation improved by geosynthetic-encased columns. *Geotext Geomembr* 32:10–17

Publisher's Note Springer Nature remains neutral with regard to jurisdictional claims in published maps and institutional affiliations.